Extreme Mechanics Letters 48 (2021) 101372

Contents lists available at ScienceDirect

Extreme Mechanics Letters

journal homepage: www.elsevier.com/locate/eml

Machine-learning based design of digital materials for elastic wave control

Jingyi Zhang[1], Yiwen Li[1], Tianyu Zhao, Quan Zhang, Lei Zuo, Kai Zhang *

School of Aerospace Engineering, Beijing Institute of Technology, Beijing, 100081, China

ARTICLE INFO

Article history:
Received 3 February 2021
Received in revised form 22 May 2021
Accepted 27 May 2021
Available online 2 June 2021

Keywords:
Structural genome
Digital material
Machine learning
Elastic wave control

ABSTRACT

Materials for wave control need to be both anisotropic and spatially distributed. Traditional method is to first design a microstructure with anisotropic property, and then change geometric parameters of the microstructure according to analytical theory or numerical calculation. Unlike the traditional method, mechanical properties of digital materials can be easily tuned by changing the 0/1 ordering without changing the geometry of digital materials. However, determining suitable orderings of digital materials according to target properties remains a key challenge. In this paper, we establish a digital structural genome to solve this problem. By combining the developed machine learning method with finite element method, we can quickly calculate elastic wave properties of digital materials with all orderings and finally establish a digital structural genome quickly and accurately. The complete digital structural genome provides us with a fast approach to design anisotropy and spatial distribution of materials. Our research unequivocally shows that the establishment of a complete structural genome database of digital materials is of great significance for inverse design multifunctional structures, and can opens an avenue to achieve wave control on demand, such as corner cloak and acoustic carpet cloak.

1. Introduction

Wave control has been widely used in different areas, such as vibration isolation [1,2], wave guiding/modulation [3–6], sub-wavelength lensing [7], focusing [8] and cloaking [9–11]. To achieve complex wave control, mechanical properties of materials in functional structures need to be both anisotropic and distributed spatially [9,10,12]. To realize the required mechanical properties, traditional method is to first design a microstructure with anisotropic property, and then gradually change geometric parameters of the microstructure according to analytical theory or numerical calculation [4,8]. Unlike the traditional method, the method based on digital materials provides a new designing way for wave control [13–16]. The representative volume element (RVE) of digital materials consists of two different unit cells (0/1-bit unit cell). By introducing the 0/1 ordering of RVE as a new designing degree of freedom, the anisotropic and spatially distributed properties of materials can be easily obtained by changing the ordering of a RVE without changing the geometric parameters [15,16]. If it is possible to quickly determine a suitable ordering of digital materials according to the target properties, functional structures for elastic wave control can be built by using discretized digital materials with different orderings, as shown in Fig. 1a. However, the relations between orderings of digital materials and their corresponding properties are not analytical, it is infeasible to use analytical methods to find suitable orderings. Numerical methods, such as finite element method and optimization method, would be time-consuming and difficult for determining a large quantity of orderings. So far, determining the orderings of digital materials according to required properties remains a key challenge.

With advancements in computing technology, machine learning (ML) has been developed to fit mapping between complex and multidimensional data [17,18]. While ML has already been successfully applied to computer science [19,20], medicine [21], and autopilot [22], it rises to prominence only recently in material science. Numerous properties of crystals and molecular structures, including the glass transition temperature [23], modulus [24,25], bandgap [26,27], and topological invariants [28–30], have been predicted by using machine learning models. However, ML method has not been used to investigate the effect of different orderings of digital materials on their mechanical properties. In this paper, a digital structural genome containing a one-to-one correspondence between orderings and mechanical properties of materials is established by a data-driven ML method with high accuracy. First, data sets which contain digital materials with different orderings and their corresponding wave properties are generated by finite element method (FEM). Then, a designed ML

* Corresponding author.
E-mail address: zhangkai@bit.edu.cn (K. Zhang).
[1] These authors contribute equally to this work.

https://doi.org/10.1016/j.eml.2021.101372
2352-4316/

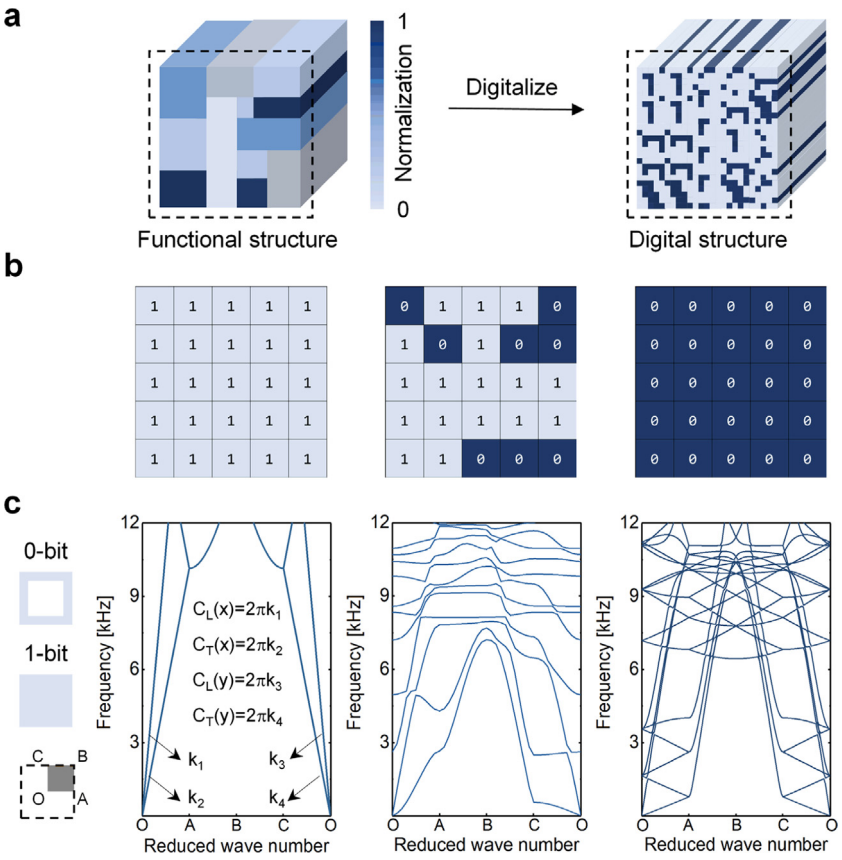

Fig. 1. Definition and application of digital materials. (a) Discretize functional structure into the structure composed of digital materials. (b) RVEs of digital materials with three different orderings. (c) Dispersion curves of RVEs with different orderings.

model is trained by feeding the data set. Using the well-trained ML model, we predict wave properties of digital materials with all orderings to finally establish a complete digital structural genome. By using the digital structural genome, digital materials with suitable orderings can be quickly found to realize complex and precise wave control, such as corner cloak and carpet cloak.

2. Methods

2.1. Generating data by FEM

Digital materials with size of 5 × 5 are shown in Fig. 1b. Two different unit cells are shown in Fig. 1c, which are composed of PLA (Young's modulus, Poisson's ratio, density are 3.5 GPa, 0.36, 1250 kg/m^3, respectively). The stiffness and density of one unit cell (10 mm × 10 mm square entity) are 3.5 GPa and 1250 kg/m^3, and the stiffness and density of another (10 mm × 10 mm square embedded with a 9.6 mm × 9.6 mm cavity, 0.2 mm wall thickness) are 0.06 GPa and 98 kg/m^3. The unit cell with large stiffness and density is chosen as 1-bit, and another is 0-bit. To obtain stronger anisotropy, we not only remove the thin wall but also increase the size of orderings. Another digital material composed of aluminum is designed with the size of 40 × 40. More details of 40 × 40 digital materials could be found in **Supplementary Information**. We combine COMSOL Multiphysics 5.5 to design a program of generating samples for training and testing. Since the sample space of 5 × 5 digital materials obeys 25-fold Bernoulli distribution, samples for training must follow the same distribution as the sample space. The program automatically generates RVEs according to the required distribution and then calls COMSOL to calculate dispersion curves of each RVE. Free triangular element is used to mesh RVEs. Bloch periodic conditions are applied to all boundaries of RVE. The slopes of the first and second acoustic branches in dispersion curves represent the wave velocities of quasi-transverse wave and quasi-longitudinal wave. The program calculates and extracts the values of slopes in dispersion curves along different three directions, including *X*-axis, *Y*-axis and 45° directions. Finally, wave velocities of digital materials with the corresponding orderings could be saved as data sets. For 5 × 5 digital materials, 50,000 samples are used for training and 10,000 samples for testing. For 40 × 40 digital materials, 150,000 samples are used for training and 30,000 samples for testing.

2.2. Building ML model

Convolutional neural networks (CNNs) are applied to fit the mapping between orderings and wave properties. Google's deep learning framework TensorFlow 1.7.0 is used to build the ML model [31]. The structure of the ML model, which consists of nine convolutional layers and three fully connected layers, is shown in Fig. 2b. To ensure that outputs have the same dimensions as inputs, both convolution kernels with the size of 3 × 3 and "SAME" padding are used after each convolution. Details of the ML model can be found in the **Supplementary Information**. Six different models are built for longitudinal/transverse wave velocities along *X*-axis, *Y*-axis and 45° directions. All variable parameters of the ML model are determined by minimizing the mean relative error (MRE) between wave velocities calculated by FEM and outputs by the ML model. To further optimize the ML model, it is necessary to avoid overfitting and ensure convergence. Here, we propose two key operations: dropout functions are used between the last three fully connected layers, while learning rate is set as

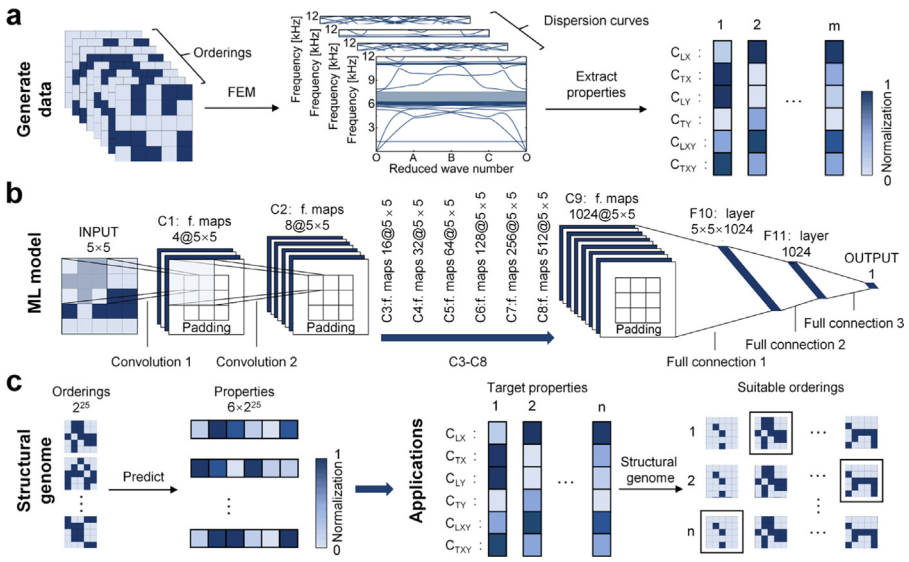

Fig. 2. Complete process of the proposed machine learning method. (a) Using FEM to calculate dispersion curves of digital materials, and extracting wave velocities from dispersion curves at longwave limit. (b) ML model consisting of nine convolutional layers and three fully connected layers to fit mapping from orderings to wave properties. (c) Using the well-trained ML model to generate a digital structural genome. Selecting materials with suitable orderings from the digital structural genome according to target properties.

an exponential decay function instead of a constant or linear function. The training process can be found in **Supplementary Fig. 1**.

10,000 samples from the testing set are fed into the well-trained ML models to verify accuracy of the ML model. The MRE for longitudinal/transverse wave velocities along the X-axis, Y-axis and 45° directions are all less than 1.5%. The testing results are shown in **Supplementary Fig. 1**. Based on testing, we find that it takes only 0.27 s to predict the wave properties directly from the ordering by using the well-trained ML model, while the FEM needs about 1000 s to obtain them under the same condition of computing power, approximately 3700 times the time taken by the ML model.

2.3. Generating digital structural genome

Since the well-trained ML model is significantly more efficient than FEM in calculating wave properties, a complete digital structural genome can be generated. First, we use permutation function to generate all orderings (2^{25}) and save them as files. Then, above files are automatically imported into the well-trained ML model to obtain corresponding properties. All orderings and their properties compose a complete digital structural genome. It takes about 6 days to generate the digital structural genome by using a computer, whose CPU, RAM and GPU are Intel Xeon Gold 6154, 1 TB and NVIDIA GeForce RTX 2080, respectively. As shown in Fig. 2c, we can obtain the most suitable orderings by searching the minimal relative error between target wave properties and data in our digital structural genome.

3. Results

3.1. Characteristics of structural genome

In the digital structural genome, the wave properties of digital materials with all orderings (2^{25}) are plotted in Fig. 3a–c. The density of 5 × 5 digital materials can be adjusted from 192 kg/m^3 to 1250 kg/m^3. Wave velocity of longitudinal wave along X-axis changes from 888 m/s to 2127 m/s, while that along Y-axis directions varies from 897 m/s to 2130 m/s. Similarly, wave velocity of transverse wave can be changed from 66 m/s to 975 m/s along X-axis and from 62 m/s to 1004 m/s along Y-axis. The minimum wave velocities of longitudinal and transverse waves along 45° directions are 742 m/s and 975 m/s, which can be tuned to 2127 m/s and 1025 m/s, respectively. Compared with traditional methods, the method using digital structural genome can design properties by changing orderings of 0/1-bit unit cells, when ratio of 0/1-bit unit cells is fixed. For example, when the ratio is 1.5 (15 1-bits and 10 0-bits), wave velocities of longitudinal wave along X-axis can be changed from 888 m/s to 1791 m/s.

The relations between orderings and their corresponding properties are governed by Christoffel equation, where Γ_{im}, ρ, c is Christoffel acoustic tensor, static effective density, wave velocity, respectively. $\left(\Gamma_{im} - \rho c^2 \delta_{im}\right) u_m = 0$. It is noted that, when the materials become anisotropic, the mode shapes are quasi-transverse and quasi-longitudinal modes, respectively. The method of determining and separating modes of anisotropic materials could be found in **Supplementary Information**. We could derive the effective elastic tensor at longwave limit through Christoffel equation when wave velocities of quasi-transverse and quasi-longitudinal wave are obtained. More details about the derivation could be found in **Supplementary Information**. Slowness profiles in Fig. 3d show effective elastic tensors of 5 × 5 digital materials. For 40 × 40 digital materials, their slowness profiles are shown in Fig. 3e and f. Each closed curve in the Fig. 3d–f represents the anisotropy of digital material with a certain ordering. When the slowness profile is almost circular, the effective elastic tensor tends to be isotropic. The greater the difference between the direction of group velocity and wavevector, the stronger the anisotropy of the materials. We define $R = C_{11}/C_{22}$ to characterize degree of anisotropy, where C_{11}, C_{22} is the stiffness along X-axis and Y-axis, respectively. For 5 × 5 digital materials, $R \approx 1$. This is consistent with the results shown in Fig. 3d, where slowness profiles are almost circular. For 40 × 40 digital materials, $0.0011 < R < 985.2170$. As seen in Fig. 3e and f, some slowness profiles are no longer circular. In the following functional design, according to the required distribution of elastic tensor and density, we could find orderings with matched properties in digital structural genome through Christoffel equations.

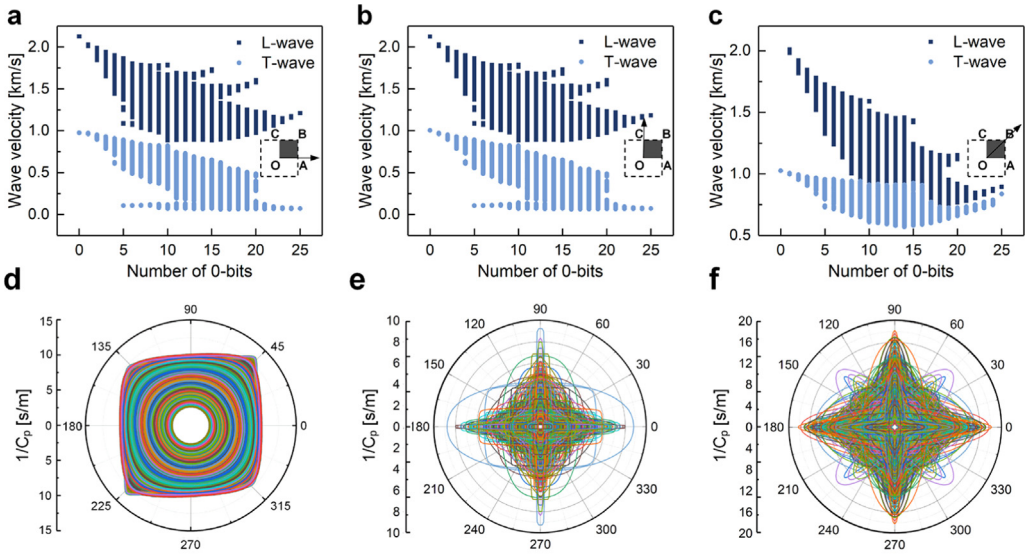

Fig. 3. Structural genome. (a) Velocities of longitudinal and transverse waves with varying numbers of 0-bits along the X-axis (a), Y-axis (b), 45° direction (c). (d) Slowness profiles of 5 × 5 digital materials (L-wave). (e) Slowness profiles of 40 × 40 digital materials (L-wave). (f) Slowness profiles of 40 × 40 digital materials (T-wave).

3.2. Wave control by designing anisotropy of materials

The digital structural genome established by the proposed method makes it easy to design functional structures for wave control. We control the propagated direction of energy, i.e., the direction of group velocity, which is the direction of outer norm vector of slowness profiles (Fig. 3d–f). Using anisotropic materials is an effective method to realize the wave control mentioned above. Here we use the digital structural genome to design anisotropy of materials. We consider a scenario that longitudinal wave is imposed on an internal boundary along 60° direction, and expect the direction of energy to be deflected 30°, 15° and 0°, respectively. To achieve the desired function of wave control, based on the digital structural genome, we first calculate angles between direction of group velocity and the wavevector of the imposed longitudinal wave. Then, we search three orderings of digital materials by matching the corresponding angles to 30°, 15° and 0°, respectively. Three orderings and corresponding slowness profiles are shown in Fig. 4a. For each ordering, 30 × 60 RVEs are used to compose a structure, and FEM simulation is carried out to verify the desired function of the structure. We conduct simulations in COMSOL Multiphysics 5.5. As shown in Fig. 4b. We impose a Gaussian beam with a frequency of 3 kHz along 60° direction. All boundaries of the structures are low reflection boundary (LRB). Free triangular element is used to mesh the structure. As the results shown in Fig. 4b, the angles deflect 30°, 15° and 0° in the structures composed of three different orderings, respectively, which are consistent with the angles from the slowness profiles in Fig. 4a. This indicates that we can use the digital materials with different orderings to realize deflection of energy.

Based on designing anisotropy of materials, we can further design a corner cloak, which makes an object invisible for acoustic wave. The schematic of the corner cloak is shown in Fig. 4c. We use the transformation theory to calculate parameters of the corner cloak. The transformation gradient can be written as

$$\mathbf{F} = \frac{\partial \mathbf{x}}{\partial \mathbf{X}} = \begin{bmatrix} 1 & 0 & 0 \\ 0 & \frac{b}{c} & 0 \\ 0 & 0 & 0 \end{bmatrix}$$

According to the transformation theory, the elastic tensor and density of the materials in the corner cloak can be easily derived as

$$\mathbf{C} = \kappa_0 \begin{bmatrix} \frac{c}{b} & 1 & 0 \\ 1 & \frac{b}{c} & 0 \\ 0 & 0 & 0 \end{bmatrix}$$

$$\rho' = \frac{c}{b}\rho_0$$

where κ_0 and ρ_0 are the bulk modulus and density of water, and $b/c = 2/3$. It is obvious that $R = 1.5$, which can be achieved by 40 × 40 digital materials. Therefore, we search the suitable ordering in the digital structural genome (40 × 40) according to the transformed elastic tensor and density. We use the digital material with suitable ordering to compose the triangular corner cloak, shown in Fig. 4c. Simulations are conducted in COMSOL Multiphysics 5.5 to verify the corner cloak. Simulation results are shown in Fig. 4c–d, in which a Gaussian beam with a frequency of 4.4 kHz is imposed at the left half of the upper boundary. The two bottom boundaries are free boundary, while others are plane radiation condition. The results indicate that without the corner cloak, an incident wave will be reflected at the boundary according to Snell's law. But when the corner cloak is applied, the incident wave propagates along the preset path, which forms an area that will not be detected by acoustic wave. Based on machine learning, the digital structural genome includes complete orderings which can offers enormous microstructural configuration compared with traditional methods. Therefore, when designing anisotropy of materials to control wave, we only need match the target anisotropy by searching in the digital structural genome rather than designing the microstructure of RVE.

3.3. Wave control by designing spatially distributed properties of materials

One of the most famous applications of the transformation acoustic technique is the carpet cloak. A key challenge is that material properties of carpet cloak need to be spatially distributed. Here, we combine digital structural genome with quasi-conformal transformation method to design an acoustic carpet cloak. The

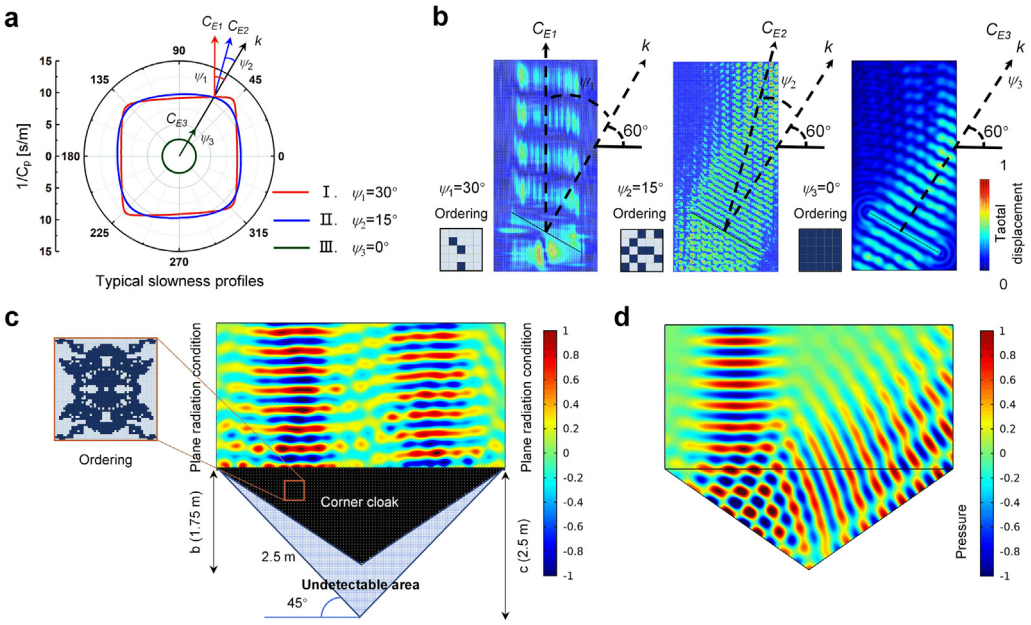

Fig. 4. Wave control by designing anisotropy of materials. (a) Three typic slowness profiles. (b) Achieving directional transmission of energy by using 5 × 5 digital materials. (c) Schematic of corner cloak, the corresponding ordering, results of corner cloak. (d). Result without corner cloak.

carpet cloak in this work is shown in Fig. 5a. The bottom-line ***BC*** is a parametric curve described by $y = 0.2\cos^{10}(\pi x/3)$, and $-0.8 \le x \le 0.8$. The lengths of the carpet cloak are ***AD*** = 2 m and ***DE*** = 1 m. First, we map the carpet cloak to the physical space, i.e., the bottom side of carpet cloak keeps as a line, and calculate the transformation gradient (Jacobian matrix) of each point in carpet cloak. According to the quasi-conformal mapping theory, the Jacobian matrix J can be obtained by solving the Laplace equation $\nabla^2\mathbf{u} = 0$ with Dirichlet boundary condition and Neumann boundary condition as

$$\begin{cases} \mathbf{n}\cdot\nabla u\,|_{ABCD,EF} = 0\,, & u\,|_{AF,DE} = x \\ \mathbf{n}\cdot\nabla v\,|_{AF,DE} = 0\,, & v\,|_{EF} = y,\quad v\,|_{ABCD} = 0 \end{cases}$$

We use the partial differential equation solver in COMSOL Multiphysics 5.5 to solve above Laplace equation. Thus, we obtain the Jacobian matrix J of each point in the transformed region. Then, according to the conformal mapping theory, the distribution of transformed density and bulk modulus can be easily obtained as

$$\begin{cases} \rho = \rho_0\sqrt{1/det\ (J)} \\ \kappa = \kappa_0\sqrt{det\ (J)} \end{cases}$$

The determinant of Jacobian matrix and its' discrete approximation are shown in Fig. 5b and e. The discrete approximation in each unit is the area average of the determinant of Jacobian matrix. To simplify the design of the cloak, we divide the transformed region into six parts as shown in Fig. 5e. For each part, we first determine the ratio of 0/1-bit unit cells in RVE according target density. Then, we determine orderings of RVE to meet the distribution of bulk modulus. The selected orderings of each part are shown in Fig. 5d. When we search orderings in the structural genome, we would choose orderings which could be connected to others directly. But it should be noticed that a few orderings may not be connected to other orderings directly, so methods in **Supplementary Information** are used to ensure the connection between different orderings. The structure composed of materials with the above orderings is shown in Fig. 5e. To verify the function of structure we designed, we carry out the simulation in COMSOL Multiphysics 5.5. The results are shown in Fig. 5c and f, in which a Gaussian beam of frequency 3.0 kHz is incident at 45° from the left side. The bottom boundary is the rigid boundary, while the other three boundaries are plane radiation conditions. Fig. 5c shows the result without carpet cloak, and it is obvious that the incident plane wave is scattered by the rigid bottom boundary. Differently, the reflected wave keeps as the plane wave and reflects along 45° when the carpet cloak composed of digital materials is used (Fig. 5f). The Cosine Similarity Index (*CSI*) is used to evaluate the performance of the carpet cloaking. *CSI* is defined as [32]:

$$CSI = \frac{\mathbf{P}^r\cdot\mathbf{P}^o}{|\mathbf{P}^r|\,|\mathbf{P}^o|} = \frac{\sum P_i^r P_i^o}{\sqrt{\sum\left(P_i^r\right)^2}\sqrt{\sum\left(P_i^o\right)^2}}$$

where $\mathbf{P}^r$ represents pressure amplitude of the rigid plane, and $\mathbf{P}^o$ represents pressure amplitude of rigid scatter with or without cloak. *CSI* ranges from −1 to 1. The larger *CSI*, the better the carpet cloaking performance. The sampling area for calculating *CSI* is marked by black dashed box in Fig. 4c and f, which is a 4 m × 2 m rectangle region. Without the carpet cloaking, *CSI* is 0.67, while with the carpet cloaking, *CSI* is 0.90. The results indicate that the designed carpet cloak possesses excellent capability of cloaking. More importantly, when the geometry of carpet cloak changes, the digital structural genome can still provide us with digital materials with suitable orderings to achieve the carpet cloak. Details of the carpet with different geometry can be found in **Supplementary Information**.

Compared with traditional methods, we only use two simple unit cells (0/1-bit) to realize distributed properties, which make a balance between the simplicity of unit cells and complexity of wave control. Digital structural genome solves the key problem of determining the suitable orderings according to the distribution of target properties. Combined with active control algorithm, our proposed method can be used as a real-time strategy to achieve novel tunable functions, such as vibration isolation, wave guiding/modulation, subwavelength lensing and focusing.

4. Conclusion

In this paper, we design a machine learning model which can be used to predict wave properties of digital materials with

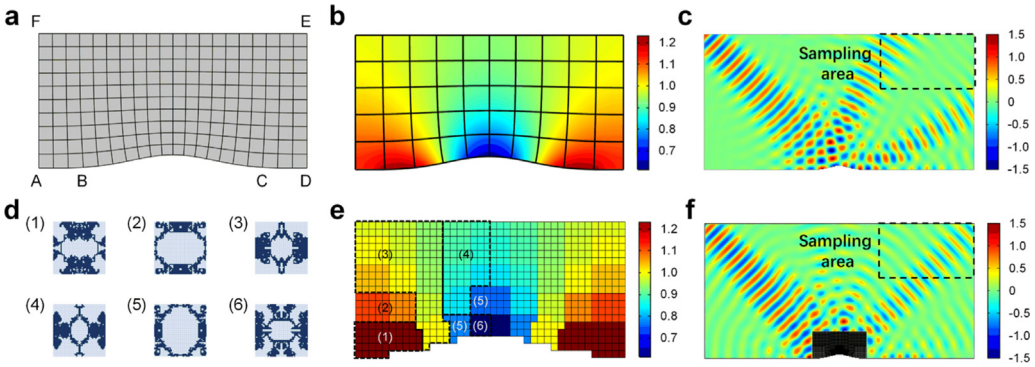

Fig. 5. Design carpet acoustic cloaking by using digital materials. (a) The schematic of carpet acoustic cloak. (b) The determinant of transformation gradient of each point. (c) Total pressure field of rigid scatter and the sampling area. (d) The selected orderings for carpet cloak. (e) The discrete approximation of the determinant of transformation gradient. (f) Total pressure field of the cloak and the sampling area.

different ordering. Based on the machine learning model, digital structural genomes are quickly established in which digital materials and their properties have a one-to-one correspondence. The digital structural genome provides us a fast approach to find digital materials with the most suitable orderings according to target properties. the proposed method can be applied to achieve some design of functional structures such as corner cloak and carpet cloak. Its high accuracy and efficiency show that the proposed method significantly reduces the time needed for inverse design, and can be used for novel tunable function with real-time strategy.

CRediT authorship contribution statement

Jingyi Zhang: Built the machine learning model, Carried out the FEM computation, Writing the paper. **Yiwen Li:** Built the machine learning model, Writing the paper. **Tianyu Zhao:** Discussed the results, Writing the paper. **Quan Zhang:** Writing the paper. **Lei Zuo:** Discussed the results, Writing the paper. **Kai Zhang:** Proposed the key idea of this paper, Writing the paper.

Declaration of competing interest

The authors declare that they have no known competing financial interests or personal relationships that could have appeared to influence the work reported in this paper.

Data availability

The authors declare that all other relevant data supporting the findings of this study are available within the Article and its Supplementary Information files, or from the corresponding author upon reasonable request.

Acknowledgments

This work has been supported by the National Natural Science Foundation of China (Grants No. 11991030 and No. 11991031).

Appendix A. Supplementary data

Supplementary material related to this article can be found online at https://doi.org/10.1016/j.eml.2021.101372.

References

[1] Z. Liu, et al., Locally resonant sonic materials, Science 289 (2000) 1734–1736.
[2] J. Mei, et al., Dark acoustic metamaterials as super absorbers for low-frequency sound, Nat. Commun. 3 (2012) 756.
[3] X. Jiang, et al., Convert acoustic resonances to orbital angular momentum, Phys. Rev. Lett. 117 (2016) 034301.
[4] Y. Xie, et al., Wavefront modulation and subwavelength diffractive acoustics with an acoustic metasurface, Nat. Commun. 5 (2014) 5553.
[5] R. Zhu, et al., Negative refraction of elastic waves at the deep-subwavelength scale in a single-phase metamaterial, Nat. Commun. 5 (2014) 5510.
[6] Y. Liu, et al., Source illusion devices for flexural lamb waves using elastic metasurfaces, Phys. Rev. Lett. 119 (2017) 034301.
[7] M. Ambati, N. Fang, C. Sun, X. Zhang, Surface resonant states and superlensing in acoustic metamaterials, Phys. Rev. B 75 (2007) 195447.
[8] S. Zhang, L. Yin, N. Fang, Focusing ultrasound with an acoustic metamaterial network, Phys. Rev. Lett. 102 (2009) 194301.
[9] S.A. Cummer, D. Schurig, One path to acoustic cloaking, New J. Phys. 9 (2007) 45.
[10] S. Zhang, C. Xia, N. Fang, Broadband acoustic cloak for ultrasound waves, Phys. Rev. Lett. 106 (2011) 024301.
[11] Y. Chen, et al., Broadband solid cloak for underwater acoustics, Phys. Rev. B 95 (2017) 180104.
[12] A.N. Norris, Acoustic cloaking theory, Proc. R. Soc. Math. Phys. Eng. Sci. 464 (2008) 2411–2434.
[13] C. Della Giovampaola, N. Engheta, Digital metamaterials, Nat. Mater. 13 (2014) 1115–1121.
[14] L. Zhang, et al., Breaking reciprocity with space–time-coding digital metasurfaces, Adv. Mater. 31 (2019) 1904069.
[15] Z. Wang, Q. Zhang, K. Zhang, G. Hu, Tunable digital metamaterial for broadband vibration isolation at low frequency, Adv. Mater. 28 (2016) 9857–9861.
[16] H. Liu, Q. Zhang, K. Zhang, G. Hu, H. Duan, Designing 3D digital metamaterial for elastic waves: from elastic wave polarizer to vibration control, Adv. Sci. 6 (2019) 1900401.
[17] Y. LeCun, Y. Bengio, G. Hinton, Deep learning, Nature 521 (2015) 436–444.
[18] M.I. Jordan, T.M. Mitchell, Machine learning: Trends, perspectives, and prospects, Science 349 (2015) 255–260.
[19] K. He, X. Zhang, S. Ren, J. Sun, Delving deep into rectifiers: surpassing human-level performance on imagenet classification, in: Proceedings of the IEEE International Conference on Computer Vision, IEEE, 2015, pp. 1026–1034.
[20] D. Silver, et al., Mastering the game of go without human knowledge, Nature 550 (2017) 354–359.
[21] R.C. Deo, Machine learning in medicine, Circulation 132 (2015) 1920–1930.
[22] M. Bojarski, et al., End to end learning for self-driving cars, 2016, arXiv: 1604.07316.
[23] D.R. Cassar, A.C.P.L.F. de Carvalho, E.D. Zanotto, Predicting glass transition temperatures using neural networks, Acta Mater. 159 (2018) 249–256.
[24] G.X. Gu, C.-T. Chen, M.J. Buehler, De novo composite design based on machine learning algorithm, Extreme Mech. Lett. 18 (2018) 19–28.
[25] O. Isayev, et al., Universal fragment descriptors for predicting properties of inorganic crystals, Nat. Commun. 8 (2017) 15679.
[26] T. Xie, J.C. Grossman, Crystal graph convolutional neural networks for an accurate and interpretable prediction of material properties, Phys. Rev. Lett. 120 (2018) 145301.

[27] S. Lu, et al., Accelerated discovery of stable lead-free hybrid organic–inorganic perovskites via machine learning, Nat. Commun. 9 (2018) 3405.
[28] Y. Zhang, E.-A. Kim, Quantum loop topography for machine learning, Phys. Rev. Lett. 118 (2017) 216401.
[29] P. Zhang, H. Shen, H. Zhai, Machine learning topological invariants with neural networks, Phys. Rev. Lett. 120 (2018) 066401.
[30] J. Carrasquilla, R.G. Melko, Machine learning phases of matter, Nat. Phys. 13 (2017) 431–434.
[31] M. Abadi, et al., TensorFlow: A system for large-scale machine learning, in: Proc. 12th USENIX Conference on Operating Systems Design and Implementation, Savannah, GA, USA, 2016, pp. 265–283.
[32] J. Xiong, T. Chen, X. Wang, J. Zhu, Design and assessment of an acoustic ground cloak with layered structure, Int. J. Mod. Phys. B 29 (2015) 1550191.